Available online at www.sciencedirect.com
ScienceDirect
Journal of Molecular Catalysis A: Chemical 267 (2007) 265–271
JOURNAL OF MOLECULAR CATALYSIS A: CHEMICAL
www.elsevier.com/locate/molcata

12-Tungstophosphoric acid supported on MCM-41 for esterification of fatty acid under solvent-free condition

Joon Ching Juan [a,b], Jingchang Zhang [b], Mohd Ambar Yarmo [a,*]

[a] *Advanced Catalysis Technology Laboratory, School of Chemical Sciences and Food Technology, Faculty of Science and Technology, Universiti Kebangsaan Malaysia, Bangi 43600, Malaysia*

[b] *Institute of Modern Catalysis, Beijing University of Chemical Technology, State Key Laboratory of Chemical Resource Engineering, Ministry of Education, Beijing 100029, China*

Received 3 August 2006; received in revised form 14 September 2006; accepted 15 September 2006
Available online 22 September 2006

Abstract

The potential of supported 12-tungstophosphoric acid (HPW) is of great importance as acid catalyst. Therefore, a series solid acid catalysts, comprised of 10–50 wt.% HPW supported on MCM-41 were synthesized and characterized using XRD, FT-IR, BET and TEM. The catalytic activities of these catalysts were tested for esterification of lauric acid with butanol using Dean-Strak apparatus, under solvent-free conditions. The host material suffers severe structural distortions at higher loading, which lead to a considerable loss of long-range orders. Based on these experimental findings, the optimal conversion of lauric acid with loading of 30 wt.% HPW was found to be higher than other loading and bulk HPW. The reaction was also studied over commercially available liquid acid, such as sulfuric acid and *p*-toluene sulfonic acid. It is assumed that the reaction mainly occurs inside the mesopores of the partially distorted MCM-41 because HPW loaded on an as-synthesized catalyst shows lower conversion than that of calcined material.
Published by Elsevier B.V.

Keywords: 12-Tungstophosphoric acid; MCM-41; Solid acid catalyst; Esterification

1. Introduction

Esterification of fatty acid with butanol, to produce fatty esters is an industrially important process. The products are mostly used as flavoring agent, solvents in cosmetics or lubricants in textile industry [1]. Esterification of fatty acid, such as lauric acid has commercially been performed using homogeneous catalyst, such as sulfuric acid and *p*-toluene sulfonic acid (PTSA). However, they are toxic, corrosive and difficult to remove from the end-product. Thus, solid acid catalysts have played an important role to overcome these problems because solid acids are less toxic, recyclable, easy to separate from the product and not corrosive. Various solid acid catalysts, such as ion-exchange resins, zeolites, sulfated zirconia and niobium acid have been used for esterification reactions [2–10]. Among these catalysts, ion-exchange resins are the most common heterogeneous catalysts used, and have proven to be effective in liquid phase esterification reactions [10]. Its disadvantage is low thermal stability, which limits the reaction temperature to 120 °C, preventing widespread use in many industries.

Besides these solid acids, the uses of stable and strongly acidic heteropoly acids, such as tungstophosphoric acid (HPW) have attracted much attention. HPW supported on various materials, such as MCM-41, activated carbon, silica, titania, resin, clay, etc., have demonstrated high catalytic activity [11–13]. MCM-41 is promising support because of its large surface area (>1000 $m^2\,g^{-1}$), high thermal stability (ca. 900 °C) and large pore size (1.5–8 nm) [14,15]. HPW cluster with ~1.2 nm diameter allows it to be introduced inside the MCM-41 pore [16]. Therefore, the large surface area of the supported HPW on MCM-41 is a potential solid acid catalyst. Besides that, its large pore size plays a major role to overcome small pores obstruct of bulky organic molecules [17]. HPW supported on MCM-41 have been tested for several esterification reactions [11,18–20]. Nevertheless, the potential of the supported HPW on MCM-41 for esterification of bulky organic molecules, such as fatty acid has not been reported.

* Corresponding author. Tel.: +60 3 89214083; fax: +60 3 89215440.
E-mail address: ambar@pkrisc.cc.ukm.my (M.A. Yarmo).

1381-1169/$ – see front matter. Published by Elsevier B.V.
doi:10.1016/j.molcata.2006.09.029

In this study, we have investigated pure siliceous MCM-41 loaded with various amount of HPW for esterification of lauric acid with 1-butanol, under solvent-free condition. We have conducted XRD, nitrogen adsorption, FT-IR, and TEM investigation to determine the effect and properties of pure siliceous MCM-41, after loaded with various amount of HPW. In addition, we have also compared the catalytic activities with those of typical liquid acids.

2. Experimental

2.1. Catalyst preparation

The pure siliceous MCM-41 material was synthesized according to the procedure reported elsewhere [21]. Cab-O-Sil M5 (fumed silica, Fluka), cetyltrimethylammonium bromide (CTMABr, Aldrich) and trimethylammonium hydroxide (TMAOH, Aldrich) 25 wt.% was used. The synthesized gels [mole composition: 0.15 CTMABr:24.3 H_2O:0.26 TMAOH:SiO_2] was transferred into Telfon-lined stainless steel autoclaves at 105 °C in static conditions for 3 days. After immediate cooling, the product was washed with deionized water until pH 8–7, filtered, and dried at 60 °C overnight. The template was removed by calcinations under nitrogen flow at 540 °C (150 cm^3 ml^{-1}) for 1 h, followed by air at the same flow rate for another 6 h.

The desired amount of HPW in aqueous solution was impregnated on MCM-41. The pH of the suspension was about 1, to avoid transformation of anion species of HPW. Then, it was stirred overnight at room temperature. After drying, the prepared catalysts were denoted by their weight percentage of HPW. For instance, 10% HPW/MCM-41 indicates the catalysts containing 10 wt.% HPW. A series of HPW/MCM-41 namely 10, 20, 25, 30, 40 and 50 wt.% were prepared according to previous method.

2.2. Commercial catalytic materials

Tungstophosphoric acid (HPW), silicotungstic acid (HSiW), *p*-toluene sulfonic acid (PTSA), Amberylst-15 and Nafion-H (NR 50, 7–8 mesh) were purchased from Sigma–Aldrich Inc. Sulfuric acid (H_2SO_4) was obtained from Fisher Scientific.

2.3. Characterization techniques

2.3.1. X-ray powder diffraction measurement

X-ray powder diffraction measurement (XRD) was performed on Bruker AXS D8 Advance using Cu Kα radiation (wavelength, $\lambda = 0.154$ nm). The samples were recorded from 1.5° to 30° (2θ) with step scan of 0.04° every 2 s.

2.3.2. Fourier transform infrared spectroscopy

FT-IR spectra were recorded on Perkin-Elmer Fourier transform infrared spectrophotometer (FT-IR) GX. The sample was pelletized with KBr and used to record the infrared spectra, ranging from 4000 to 400 cm^{-1}.

2.3.3. Textural properties

The BET surface area was performed using Micromeritics Model ASAP 2010 instrument from the nitrogen adsorption isotherms at 77 K. All samples were degassed at 100 °C under vacuum overnight. Specific surface area (S_{BET}) were calculated from the linear part by BET equation at $p/p_0 = 0.05$–0.30. Average pore diameter (D_{pore}) and pore volume (V_{pore}) was calculated based on Barret–Joyner–Halenda (BJH) method.

2.3.4. Transmission electron microscopy

Transmission electron microscopy (TEM) was performed on Super Twin Philips Technai 20 transmission electron microscope equipped with field emission gun operated at 200 kV. The samples were suspended in *n*-hexane and the suspension droplet was placed on a copper grid coated with microgrid carbon polymer (400 meshes, Agar Scientific).

2.4. Catalysis reaction

The liquid phase esterification of lauric acid (Aldrich, 99%) with 1-butanol (Fisher Scientific, 99%) was tested. The reaction was carried out using a Dean-Stark apparatus at atmospheric pressure, which equipped with a magnetic stirring bar. The reactor was charged with lauric acid 20.0 g (0.1 mol) and butanol 11.0 cm^3 (0.12 mol). Then, about 1.0 g (5 wt.% based on lauric acid) catalyst was added. The reaction temperature was slowly raised to 110–120 °C and maintained at the desired temperature during the specified reaction periods. The heating was stopped after 4 h to determine the conversion. The product was analyzed by Hewlett Packard gas chromatography (GC) 5890 model with flame ionization detector (FID). MXT-1 Crossbond 100% dimethyl polysiloxane (15 m) column was used. *n*-Tetradecane was added as an internal standard. The parameter for the temperature program: start at 150 °C (2 min), ramp at 5 °C min^{-1} to 250 °C.

3. Results and discussion

3.1. Characterization of the catalysts

3.1.1. XRD analysis

The typical XRD patterns of MCM-41 are shown in Fig. 1(a). According to Beck et al. [22], MCM-41 has an intense peak with two peaks that could be indexed to (1 0 0), (1 1 0) and (2 0 0) planes. Its unit cell, $a = 4.50$ nm ($a = 2d_{100}/\sqrt{3}$) and d_{100} is 3.90 nm ($d = n\lambda/2 \sin\theta$). The geometry of MCM-41 hexagonally unit cell is $a = b$ and c = infinite. XRD patterns of MCM-41 have a limited number of reflections and all peaks are situated at low angles. This is because a and b parameters are in the order of nm instead of tenths of nm.

The effect of HPW loading is also depicted in Fig. 1. As shown in Fig. 1(h), physically mixed samples display HPW reflection patterns, which due to inhomogeneous distribution of HPW on MCM-41. Considering the XRD detection limit, it can be assumed that the size of HPW crystals is at least 10 nm [19]. Upon loading the HPW to 30 wt.%, no reflection patterns corresponding to HPW was observed (Fig. 1(e)). Therefore, it

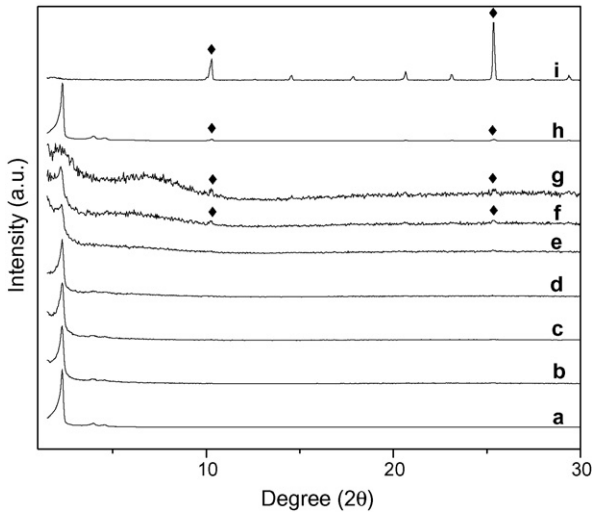

Fig. 1. XRD patterns of (a) MCM-41, (b) 10% HPW/MCM-41, (c) 15% HPW/MCM-41, (d) 25% HPW/MCM-41, (e) 30% HPW/MCM-41, (f) 40% HPW/MCM-41, (g) 50% HPW/MCM-41, (h), physically mixed (20 wt.% HPW), and (i) HPW. (♦) The crystal phase of HPW.

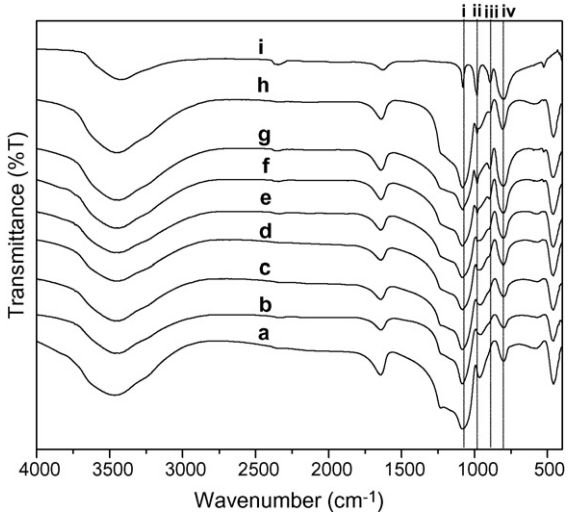

Fig. 2. FT-IR spectra of (a) MCM-41, (b) 10% HPW/MCM-41, (c) 15% HPW/MCM-41, (d) 25% HPW/MCM-41, (e) 30% HPW/MCM-41, (f) 40% HPW/MCM-41, (g) 50% HPW/MCM-41, (h) physically mixed (20 wt.% HPW), and (i) HPW.

is assumed that HPW is well dispersed on MCM-41. Since, the MCM-41 used has a pore size of 3 nm, these HPW crystals (∼1.2 nm) is expected to be found inside the support. This result is not surprising because physically mixed HPW tends to agglomerate on the outer surface, as compared to well-dispersed HPW in the aqueous solution before impregnation. However, at loading over 40 wt.%, bulk HPW crystals give rise to reflection at $2\theta = 10.3^\circ$ and 25.4°. This is indicative of poor dispersion of HPW at loading above 40 wt.%. It is assumed that HPW was not just well dispersed but located inside the pores of MCM-41 for less than 30 wt.% loading.

Furthermore, at these high loading, the HPW has a striking effect on the width and intensity of the main reflection at d_{100} spacing, and this line becomes broader and weaker as the loading increases. Although the reflection is severe at loading above 40 wt.% but the MCM-41 reflection could still be observed. It is indicated that MCM-41 long-range order is significantly decreased by the presence of HPW. The effect on the MCM-41 with presence of HPW are similar to those reported by other authors [23,24], but little explanation regarding this phenomenon was discussed. They are three reasonable explanations causing striking effect on the width and intensity of XRD reflection. First, the hydrolysis of MCM-41 may cause the collapsed of hexagonal framework. The siloxane (Si–O–Si) group of MCM-41 is easily hydrolyzed by water to hydroxyl (Si–OH) group. The resulting terminal OH groups (Si–OH) on the surface make MCM-41 even more easily to be attacked by hydroxide ion of water, leading consequently to the partial destruction of mesoporous structure. Second, it may due to an interaction between anion species of HPW, such as $[PW_{12}O_{40}]^{3-}$, $[P_2W_{21}O_{71}(H_2O)_3]^{6-}$ or $[P_2W_{18}O_{62}]^{6-}$ and silanol group inside the wall and pore of MCM-41 [14,24]. Third, the intensity reduction at d_{100} could be due to radiation absorption by the tungsten element present in HPW [25]. As shown in Fig. 2(h), the physically mixed exhibits a clear peak at d_{100}, d_{110} and d_{200} without distorted pattern. Moreover, there is no significant effect on width and intensity observed. For that reason, the distortion pattern and reduced of intensity of the strongest d_{100} diffraction peak in the case of the HPW impregnated material causes by radiation absorption of tungsten element is negligible.

In general, siloxane linkage is rapidly hydrolyzed under strong acidic conditions. Further, to study the stability of MCM-41 under acidic conditions, the MCM-41 material was stirred overnight in 0.1 M HCl solution and water. The main reflection at d_{100} of MCM-41, stirred under acid conditions was much broader than MCM-41 stirred under aqueous conditions. The results proved that MCM-41 is readily hydrolyzed in water and more severe under acidic conditions. It is assumed that the severe reflection of MCM-41 at loading above 40 wt.% is mainly due to the loss of long-range order. The results show good agreement with the other literatures reported earlier [26,27]. They reported that mesoporous structure of Si–MCM-41 collapsed in hot water and aqueous solution due to silicate hydrolysis.

3.1.2. FT-IR spectroscopy

FT-IR spectra of pure HPW in the region of 1500–400 cm^{-1} are shown in Fig. 2(d). The four main absorption assigned for pure bulk HPW were observed at (i) 1080 cm^{-1} (P–O_a), (ii) 983 cm^{-1} (W=O_d), (iii) 893 cm^{-1} (W–O_b–W) and (iv) 800 cm^{-1} (W–O_c–W) [24], are ascribed to asymmetric bond stretching vibration. Fig. 2(a) shows a broad band around 3426 cm^{-1} assigned to OH stretching vibration of MCM-41, which could be associated to Si–OH and water vibration. Despite that, a broad band around 1300–1000 cm^{-1} of the support is assigned to asymmetric stretching mode of Si–O–Si. Two more bands at 801 and 458 cm^{-1} are due to symmetric stretching vibration and bending vibration of rocking mode of Si–O–Si respectively. The band at 966 cm^{-1} is assigned to the presence of Si–OH symmetric stretching vibration. Although, an overlapping of certain bands from MCM-41 material with HPW, the

Table 1
Adsorption data on MCM-41 and HPW/MCM-41

Sample	S_{BET} ($m^2\,g^{-1}$)	V_{pore} ($ml\,g^{-1}$)	D_{pore} (nm)
MCM-41	1071	0.82	3.08
10% HPW/MCM-41	611	0.33	3.00
15% HPW/MCM-41	545	0.30	2.99
25% HPW/MCM-41	321	0.17	3.14
30% HPW/MCM-41	294	0.16	3.26
40% HPW/MCM-41	191	0.12	3.60
50% HPW/MCM-41	74	0.07	4.87
HPW	5[a]	–	–

[a] Reported value from Ref. [24].

information could still be observed from less affected regions. The less affected regions are at 983 cm^{-1} and a small band at 893 cm^{-1}. Additionally, Fig. 2(h) shows the physically mixed has a clear band at 983 and 893 cm^{-1}. This evidence the presence of intact Keggin anion because HPW will not decomposed by physically mixing. These peaks became more evidence with increase of HPW loading, due to greater number of oscillators. It is suggested that HPW is still intact, after supported on MCM-41. Moreover, there is no shift of W=O_d band occurred after impregnation, as shown in Fig. 2(b–g). There are no peaks observed at 1085 and 1040 cm^{-1}, which are assigned to $[PW_{11}O_{39}]^{7-}$ [24]. This is because this species usually present when pH higher than 2 [28,29]. There are some transformation appear at pH less than 1 [28,29], such as $[P_2W_{21}O_{71}(H_2O)_3]^{6-}$, $[P_2W_{18}O_{62}]^{6-}$ and $[P_2W_{20}O_{70}]^{10-}$, but the major species is still $[PW_{12}O_{40}]^{3-}$.

3.1.3. Surface and porosity

The textural properties of MCM-41 are listed in Table 1. The wall thickness of parent MCM-41 is 1.42 nm (calculated from the difference between unit cell measurement obtained from XRD reflection peak at d_{100} and pore diameters calculated from N_2 adsorption). The surface area and pore volume of the catalyst significantly decreased with increasing the HPW loading. The pore size remains as the loading increase but at loading above 40 wt.%, the pore size is drastically enlarged. These facts lead us to assume that HPW is located inside the pore and pore blockage did not take place. However, the drastic pore enlargement is due to loss of MCM-41 long-range order. The results parallel with XRD that the severe distortion pattern as the loading increase is due to loss of long-range orders.

Adsorption isotherms of MCM-41 samples, before and after impregnation are shown in Fig. 3. The typical curve of parent MCM-41 sample of mesoporous material could be assigned to type IV isotherm. There is a dropped in the adsorption condensation region, at $p/p_0 = 0.3$–0.4 for the supported HPW. It is expected that HPW species occupied and dispersed on MCM-41 surface causes the dropped in the adsorption region. Moreover, at loading below 30 wt.%, mesoporous isotherm (type IV) characteristic still could be observed, but the condensation region beginning to disappear at higher loading.

3.1.4. TEM analysis

TEM image of MCM-41 is illustrated in Fig. 4(a). The image shows a long stripe, which could be the long-range order or

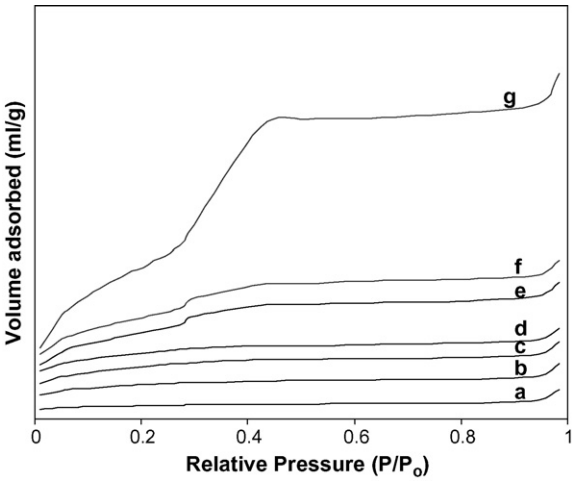

Fig. 3. Nitrogen adsorption isotherm of (a) 50% HPW/MCM-41, (b) 40% HPW/MCM-41, (c) 30% HPW/MCM-41, (d) 25% HPW/MCM-41, (e) 15% HPW/MCM-41, (f) 10% HPW/MCM-41 and (g) MCM-41.

channel of hexagonal order material. However, after HPW was supported on MCM-41, the long-range order of MCM-41 is unseen (Fig. 4(b)). It is showing good agreement with XRD and nitrogen adsorption results that the loss of long-range order is due to hydrolysis of MCM-41 wall. Nonetheless, at loading below 30 wt.%, the XRD and nitrogen adsorption results still show an evidence of MCM-41 mesoporous structure.

If HPW is present, a darker spot could be observed, because HPW comprised of tungsten element. However, it is undeniable that image of parent MCM-41 show several darker spots due to stacking of the particles. As shown in Fig. 4(b), there is no clear sign of bulk HPW species located outside the edge of MCM-41 particles. Although the long-range order was partially turned amorphous, the HPW is well dispersed and located inside the pores of MCM-41.

3.2. Catalyst testing for esterification of lauric acid

3.2.1. Effect of HPW loading on MCM-41

The effect of HPW loading on MCM-41 for esterification of lauric acid is shown in Fig. 5. It is obvious that the conversion of the prepared catalyst increases with increasing loading of HPW to a maximum at 30 wt.%. Further increase in HPW loading resulted in a decrease in catalyst performance. The conversion of 30% HPW/MCM-41 is higher than that of parent bulk HPW. Moreover, TOF of the supported HPW is higher than that of bulk HPW. It is suggested that the enhancement is due to well dispersion of HPW on MCM-41. Although we cannot exclude the presence of small amount of other polyanions, we have no direct evidence of this. FT-IR spectra are consistent with the spectra reported [24] for HPW systems. At this stage, we cannot exclude a role for the enhanced catalytic activity arising from the interaction between surface silanol and anion of HPW, to produce stronger acidity sites for the reaction [14,24]. In this study, the correlation among spectroscopic (FT-IR), XRD, surface area, porosity, and catalyst performance results suggests that enhanced of catalytic activity is mainly due to well

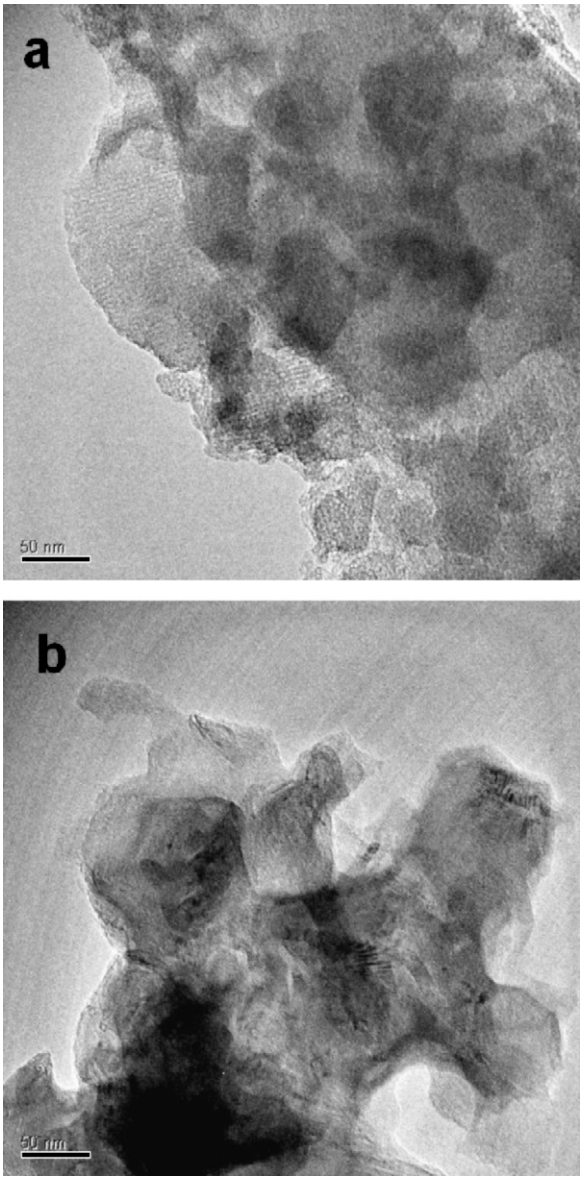

Fig. 4. TEM image of (a) MCM-41 and (b) 30% HPW/MCM-41.

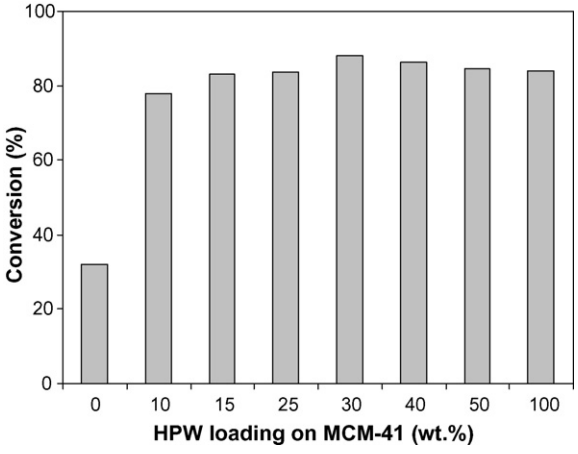

Fig. 5. Catalytic activities of HPW loading on MCM-41 for esterification of lauric acid.

Table 2
Catalytic activity of the different catalysts for esterification of lauric acid and butanol

Entry	Catalyst	Conversion (%)	TOF[a] (min^{-1})
1	H_2SO_4	93	0.04
2	Bulk HSiW	88	0.30
3	PTSA	87	0.07
4	Bulk HPW	81	0.89

[a] Turn over frequency (TOF) was calculated as the mole ratio of ester formed over mole of active sites per minute. Mole of active sites is based on mass of samples over molecular weight.

dispersion of HPW. Hence, the partially destroyed long-range order could also ease the diffusion resistance of bulky molecules, such as lauric acid into the active sites. At loading above 40 wt.%, the low catalytic activity is due to the poor dispersion of HPW on MCM-41. Besides that, the low surface area for loading above 40 wt.% is also contributed to the drop of catalytic activity.

Further, the study was also tested with 30 wt.% HPW loaded on as-synthesized MCM-41. The conversion found to be lower for as-prepared catalyst. Therefore, this suggests that the reaction occurs mainly within the pores, as this catalyst is unable to allow the diffusion of the reactant inside the pore due to template blocking. A 62% conversion obtained, which is 27% less than that of HPW loaded on calcined sample. It is assumed that the reaction took place within the pores of MCM-41, rather than on the outer surface. This indirectly proved that HPW is situated inside the pores of MCM-41. A 36% conversion obtained with Nafion-H, which is only 4% more than that of no catalyst was added into the reaction. It is concluded that Nafion-H is not an effective solid acid catalyst because the small pores and low surface area ($0.02\ m^2\ g^{-1}$) obstruct access of bulky molecules to it active sites for reaction to take place.

3.2.2. Catalytic activity of different catalysts

The activity of bulk heteropoly acids, sulfuric acid (H_2SO_4) and *para*-toluene sulfonic acid (PTSA) is shown in Table 2 (entries 1–4). In esterification of lauric acid, sequences of conversion over homogeneous catalysts decreased in the following order: $H_2SO_4 > HSiW \sim PTSA > HPW$. Meanwhile, TOF orders is as follows: $HPW \gg HSiW \gg PTSA > H_2SO_4$. The result reveals that HPW is more efficient catalysts than other homogeneous catalysts. It was reported in the literature [11], that acid strength of heteropolyacids, especially HPW is stronger than H_2SO_4 and PTSA. Therefore, this help to explain the higher activity of HPW in the reaction, is mainly due to stronger acidity.

3.2.3. Effect of reaction time

The effect of reaction period on the esterification was studied on 30% HPW/MCM-41 catalyst. The reaction was carried out without using any extra solvent, such as toluene to promote more environmentally friendly reaction. It is found that azeotropic distillation is also possible with some excess of butanol. After condensation, water separated from the organic phase, which was then recycled back to the reaction. Although, there is no doubt, the conversion will keep increasing after 4 h toward completion, but due to industrial concern, a rapid production is

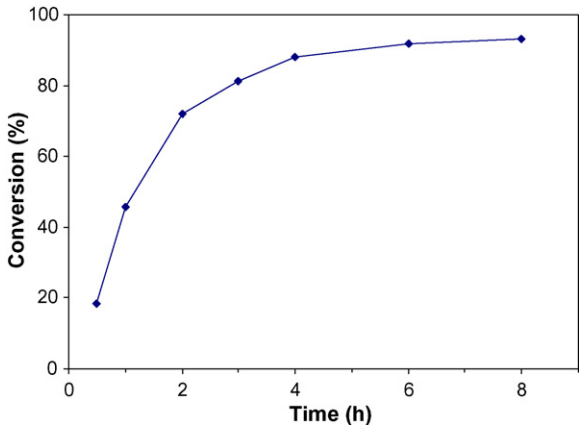

Fig. 6. Effect of time over 30% HPW/MCM-41 for esterification of lauric acid.

substantial for economical benefit. Therefore, if esterification reaction is prolonged, the catalyst is considered extravagant to be used in industry. Fig. 6 shows the conversion of lauric acid increases rapidly in the beginning and gradually levels off after 4 h. For instance, the conversion from around 18% in the first 30 min to around 81% in 3 h; on increasing the reaction time to 4 h, the conversion increased only to 88%.

3.2.4. Reusability of the catalysts

Reusability of 30% HPW/MCM-41 and Amberlyst-15 is depicted in Fig. 7. The catalyst recovered by filtration and served for next esterification. The 30% HPW/MCM-41 shows high conversion for initial reaction, but the reusability decreased as compared to Amberlyst-15. During fourth times of reuse, conversion of lauric acid catalyzed by 30% HPW/MCM-4 was significantly decreased to 40%. Perhaps, the loss of activity is due to leaching and dissolution of the supported HPW during reaction. To verify dissolution of the supported HPW during reaction, the product was filtrated and analyzed by using inductively coupled plasma-optical emission spectroscopy (ICP-OES). The weight of W in the solution during first, second, third, fourth and fifth time of reuse is 0.0483, 0.0162, 0.0306, 0.0384, and 0.0264 g. Although, as reported by several authors that there is interaction of silanol group with HPW [14,16,24].

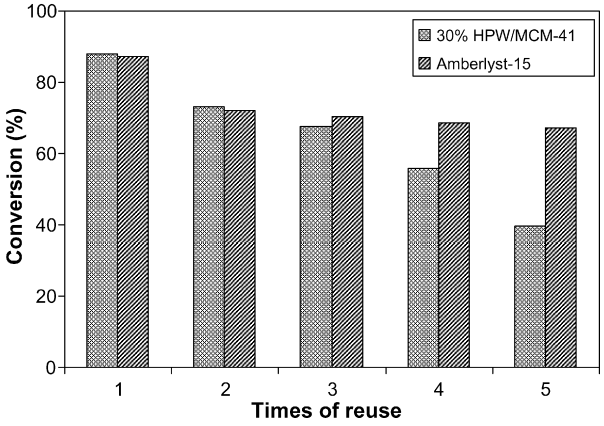

Fig. 7. Reuse of 30% HPW/MCM-41 and Amberlyst-15 catalyst in esterification of lauric acid.

However, it should be note that HPW is still readily dissolved during reaction. This indirectly demonstrated that the interaction between silanol groups of MCM-41 and HPW is weak. Recently, it was reported that HPW was not just dissolved, but also occurrence of sintering and clustering of the recycled catalyst [19,23]. If the sintering and clustering occurred, the reflection peaks corresponded to bulk HPW could be observed. During four times of reuse, no reflection peaks corresponded to bulk HPW was observed. Therefore, these facts lead us to assume that dissolution of the supported HPW is more pronounced. In addition, the structure of MCM-41 remains during four times of reuse. Amberlyst-15 shows lower catalytic than that of supported HPW at the beginning, but it activity is almost remain during four times of reuse. The reusability of Amberlyst-15 is better because the active sites (sulfonic groups) are chemical bonded on the resin.

4. Conclusion

We have shown that HPW supported on MCM-41 are active solid acid catalysts for esterification of bulky molecules, such as lauric acid. For esterification of lauric acid, the optimal loading of HPW was found to be 30 wt.%. Although, MCM-41 structure is distorted after loaded with HPW, the conversion was higher than parent HPW. The HPW/MCM-41 show excellent catalytic activity, but reusability gradually decreased as compared to Amberlyst-15. The loss of activity during four times of reuse is due to the supported HPW tends to leach and dissolve during reaction. In addition, the structure of MCM-41 remains during four times of reuse. Esterification of lauric acid over 30 wt.% HPW on as-synthesized MCM-41, demonstrated lower conversion than calcined sample. Hence, the esterification is proposed to take place inside the pores. It is showing good correlation with XRD and nitrogen adsorption that HPW was finely dispersed inside the channel of MCM-41. It is noteworthy that esterification could be carried out using solid acids under solvent-free conditions to promote greener reaction.

Acknowledgments

We are grateful to the Ministry of Science and Technology for financial (IRPA grant 09-02-02-0033) support. The authors thank UNESCO/China Great Wall Co-sponsored Program for a fellowship to J.C. Juan. We also thank Dr. Mat Hussain for the accessibility of scanning HR-TEM.

Appendix A. Supplementary data

Supplementary data associated with this article can be found, in the online version, at doi:10.1016/j.molcata.2006.09.029.

References

[1] A. Meffert, J. Am. Oil Chem. Soc. 61 (1984) 255.
[2] W.T. Liu, C.S. Tan, Ind. Eng. Chem. Res. 40 (2001) 3281.
[3] M.R. Altiokka, A. Citak, Appl. Catal. A: Gen. 239 (2003) 141.
[4] S.R. Kirumakki, N. Nagaraju, K.V.R. Chary, S. Narayanan, Appl. Catal. A: Gen. 248 (2003) 161.
[5] A. Corma, H. Garcia, S. Iborra, J. Primo, J. Catal. 120 (1989) 78.

[6] I. Hoek, T.A. Nijhuis, A.I. Stankiewicz, J.A. Moulijn, Appl. Catal. A: Gen. 266 (2004) 109.
[7] S. Ardizzone, C.L. Bianchi, V. Ragaini, B. Vercelli, Catal. Lett. 62 (1999) 59.
[8] T.S. Thorat, V.M. Yadav, G.D. Yadav, Appl. Catal. A: Gen. 90 (1992) 73.
[9] M. Hiyoshi, B. Lee, D. Lu, M. Hara, J.N. Kondo, K. Domen, Catal. Lett. 98 (2004) 181.
[10] T.A. Peters, N.E. Benes, A. Holmen, J.T.F. Keurentjes, Appl. Catal. A: Gen. 297 (2006) 182.
[11] I.V. Kozhevnikov, Chem. Rev. 98 (1998) 171.
[12] J. Haber, K. Pamin, L. Matachowski, D. Mucha, Appl. Catal. A: Gen. 256 (2003) 141.
[13] Y. Izumi, K. Hisano, T. Hida, Appl. Catal. A: Gen. 181 (1999) 277.
[14] I.V. Kozhevnikov, K.R. Kloetstra, A. Sinnema, H.W. Zandbergen, H. Van Bekkum, J. Mol. Catal. A: Chem. 114 (1996) 287.
[15] C.T. Kresge, M.E. Leonowicz, W.J. Roth, J.C. Vartuli, J.S. Beck, Nature 359 (1992) 710.
[16] I.V. Kozhevnikov, A. Sinnema, R.J.J. Jansen, K. Pamin, H. Van Bekkum, Catal. Lett. 30 (1995) 241.
[17] T. Okuhara, N. Mizuno, M. Misono, Adv. Catal. 41 (1996) 113.
[18] W. Chu, X. Yang, Y. Shan, X. Ye, Y. Wu, Catal. Lett. 42 (1996) 201.
[19] M.J. Verhoef, P.J. Kooyman, J.A. Peters, H. Van Bekkum, Micropor. Mesopor. Mater. 27 (1999) 365.
[20] L.R. Pizzio, P.G. Vazquez, C.V. Caceres, M.N. Blanco, Appl. Catal. A: Gen. 256 (2003) 125.
[21] A. Corma, A. Martinez, V. Martinez-Soria, J. Catal. 169 (1997) 480.
[22] J.S. Beck, C.T. Chu, I.D. Johnson, C.T. Kresge, M.E. Leonowicz, W.J. Roth, J.C. Vartuli, PCT Int. Appl. WO 91/11390, 1991.
[23] B.R. Jermy, A. Pandurangan, Appl. Catal. A: Gen. 295 (2005) 185.
[24] A. Ghanbari-Siahkali, A. Philippou, J. Dwyer, M.W. Anderson, Appl. Catal. A: Gen. 192 (2000) 57.
[25] P.A. Jalil, M.A. Al-Daous, A.R.A. Al-Arfaj, A.M. Al-Amer, J. Beltramini, S.A.I. Barri, Appl. Catal. A: Gen. 207 (2001) 159.
[26] L.Y. Chen, S. Jaenicke, G.K. Chuah, Micropor. Mater. 12 (1997) 323.
[27] S. Kawi, S.-C. Shen, Mater. Lett. 42 (2000) 108.
[28] Z. Zhu, R. Tain, C. Rhodes, Can. J. Chem. 81 (2003) 1044.
[29] B.J. Smith, V.A. Patrick, Aust. J. Chem. 57 (2004) 261.